Wildfire in the West: Assessing the Detectability of a Post-fire Signal at the Watershed Scale

Aaron Heldmyer[1], Ben Livneh[1,2]
[1]Department of Civil, Environmental, and Architectural Engineering, University of Colorado Boulder, Boulder, CO, 80309.
[2]Cooperative Institute for Research in Environmental Sciences, University of Colorado Boulder, Boulder, CO, 80309.

Abstract

Wildfires are expected to increase in both size and severity in the western U.S. These disasters cause important, often lasting changes to watershed dynamics, particularly in sediment mobilization processes, and create problems for downstream reservoirs and water treatment facilities. Therefore, it is essential to improve our understanding of wildfire-driven changes in streamflow and suspended sediment loading (SSL) to mitigate damages. Previous efforts to model wildfire effects have often focused on a small subset of sites and a limited number of post-fire hydrologic processes changes such that the insights gained have generally lacked transferability due to regional variations in the drivers of these responses. Additionally, scarcity of observational sediment data provides a further challenge for finding generalizable influences on post-fire sediment response useful for modeling in areas with little to no available sediment data, which represent the vast majority of basins in the West. In this research, we seek to improve understanding of post-disturbance hydrology and sedimentation by first characterizing streamflow and sediment relationships through commonly used rating curve parameters at a diverse set of gaged locations across the western U.S. We combine this with basin topographical and water infrastructure development information from the GAGES-II dataset. We then select a relatively undeveloped basin from this dataset (the Rio Puerco near Bernardo, NM) that has been affected by five observed fire events between 1999 and 2014 as a testbed for measuring the viability of a set of increasingly data-intensive approaches for finding a detectable post-fire sediment response signal. We begin by applying a statistical model to pre-fire stream gage data and forecasting the post-fire season, comparing differences in suspended sediment loading (SSL) magnitudes between the forecast and observations. We subsequently add precipitation data from Daymet (basin-averaged, then gridded), and fire extent data from the Monitoring Trends in Burn Severity (MTBS) dataset to improve post-fire sediment signal strength. Future work will see further exploration of novel detection techniques, as well as the eventual application of these methodologies to other western basins in an effort to uncover regional influences on sediment response to wildfire. This study carries implications for post-fire sediment modeling, water management, and reservoir operations.

Introduction

Wildfires are expected to increase in both size and severity in the western U.S. Sankey et al. (2017) predicts that post-fire sedimentation rates will increase by over 10% for nearly 9/10ths of watersheds, and greater than 100% for more than 1/3rd of watersheds by the 2041-2050 decade. This is cause for concern, as these disasters instigate important and often lasting changes to watershed dynamics, particularly in sediment mobilization processes, and create problems for downstream reservoirs and water treatment facilities. Recent studies have shown that post-fire overland flow, discharge, and peak flows can increase by several orders of magnitude relative to pre-fire conditions, particularly in the first 1-3 years (Neary et al., 2011). Within streams, suspended sediment particles from fire-affected locations have been known to exhibit significantly higher settling velocities than unburned particles of similar diameter due to reduced organic content and pore space (Blake, et al., 2007, 2009). As a consequence, an increase in fine sediment loading in streams and reservoirs located downstream of affected areas may be observed (Smith et al., 2011). This can necessitate costly interventions such as reservoir dredging for downstream infrastructure (Jones et al., 2017), further underscoring the importance of understanding post-fire effects on hydrology and geomorphology.

From a hydrologic standpoint, destruction of vegetation and litter following an event affects canopy interception, evapotranspiration, and storage of rainfall, which can also influence the accumulation and melting of snow (Shakesby & Doerr, 2006). Wildfire-induced soil heating affects its physical and chemical properties, increasing water repellency and decreasing aggregate stability. Rain splash can disrupt and compact the soil, and fine sediments dislodged by this process can clog soil pores and lead to surface sealing. An abundance of fine sediments generated from the ash of combusted vegetation leads to further water repellency (Meyer & Wells, 1997). Infiltration is often reduced as a result of these changes (Moody & Martin, 2001), which in turn generates considerably higher overland flow, increased discharge, and peak flows orders of magnitude greater than pre-fire conditions, particularly in the first 1-3 years (Neary et al., 2011).

The geomorphology of a basin is also affected in a variety of ways. Numerous studies have documented increased erosion rates following a fire disturbance (Benavides-Solorio & MacDonald, 2001; Cerda & Doerr, 2005; Luis, et al., 2003; Emmerich & Cox, 1994; Fernandez, et al., 2011). Since erosion is largely dependent on overland flow, erosion rates are usually determined by factors that control runoff generation: soils, vegetation, and water input. Overland flow arises from either saturation-excess or infiltration-excess conditions, and it is the latter that is the dominant mechanism in arid and semi-arid regions where wildfires are commonplace (Wondzell & King, 2003). Easily erodible sediment becomes exposed when protective vegetation cover is burned away, and a combination of soil organics combustion and intense heating leads to decreased cohesiveness of surface soil and further ease of erosion (Johansen, et al., 2001).

In addition to the spatial component of wildfire disturbance, the temporal component of how wildfire effects manifest years or even decades into the future following an event is perhaps equally as important to characterize. The impact of wildfire disturbance can be quantified by measuring the post-fire change in process rates (discharge, hillslope and channel erosion, sediment transport, and deposition) and contrasting these with pre-fire conditions (Swanson, 1981). Some studies (Vieira, et al., 2015) characterize this difference

using a logarithmic response ratio, which expresses the proportional difference in a response variable between a "treatment" (burned area) and an unburned reference. This is a typical metric for meta-analysis of ecological data.

The relationship between pre- and post-fire process rates may be observed through time. Immediately following a wildfire event, during the "initial phase", process rates have been observed to increase with time before reaching a maximum. A recovery phase then takes place following this maximum where the rates decrease. The combined length of these two phases are what is known as the *relaxation time*, which can vary widely from one to three years for sediment fluxes, up to thirty years for discharge, and longer for regrowth of trees (Rowe, et al. 1949). Over long time intervals, the importance of wildfire as a geomorphic agent depends upon the ratio between this relaxation time, and the wildfire recurrence time: a ratio known as the *transient form ratio* (Brunsden and Thornes, 1979). Because wildfires lower the threshold of energy required for erosion to take place, even a low intensity storm event coupled with spatially heterogeneous wildfire effects can be an important agent for sediment mobilization, particularly in arid and semi-arid mountainous basins common across the West (Moody & Martin, 2001).

While many experiments document the effects of wildfire on erosion and overland flow magnitudes at the plot scale, few studies (Reneau et al., 2007; Pelletier & Orem, 2014) focus on post-fire sedimentation effects at the basin scale, which is significantly more important to quantify in order to avoid costly damages for downstream reservoirs and water treatment facilities. Unfortunately, predicting sediment delivery at the basin scale is a much more complicated process than predicting at the plot or hillslope scale, due to the addition of numerous processes, sources, and sinks that may hinder or help a sediment particle in reaching the basin outlet (Fryirs, 2013). For sediment transport, it is often noted that river systems act as 'jerky conveyor belts' (Ferguson, 1981), in that sediment is transported episodically through the catchment. Landforms in which sediment may be stored for long periods of time, such as slopes, floodplains, or terraces, may attenuate or even completely mask a sediment response signal (Fryirs & Brierley, 2001). The effects of a wildfire event on sediment loading may not make themselves known at the basin outlet until months, or even years after the fact.

To further complicate the issue, there are also limited resources available for the direct observation of sedimentation in the U.S. In the West, there are over 9,000 decommissioned or active gages measuring streamflow according to the USGS Geospatial Attributes of Gages for Evaluating Streamflow (GAGES-II) dataset (Falcone, 2017). Of these, 2,317 of the gaged basins are co-located with wildfire ignition points documented in the Monitoring Trends in Burn Severity (MTBS) dataset (Eidenshink et al., 2007), and only a small subset (n = 187) also contain direct measurements of suspended sediment concentration (SSC) at any point in their operational lifetime; that is, not necessarily when a wildfire event has taken place. This paper presents a preliminary analysis into the problem of detecting the post-fire hydrologic and sediment response from basins across the western U.S. in the context of this sparse data availability, and sets the stage for future work, which will more rigorously assess the detectability of wildfire signals at the basin scale using supplemental data derived from prior studies, remotely-sensed basin physiography, and meteorological observations. We first conduct a meta-analysis of gaged basins across the West as a top-down comparative measure, and subsequently focus on a

single basin to serve as a testbed for refining several analytical techniques with the aim of uncovering a robust post-fire sediment signal.

Study Domain and Data Products

The western U.S. was selected as the study domain for evaluation of regional variations in hydrologic and geomorphologic response to wildfire, as well as in relationships between streamflow and sediment transport (Figure 1).

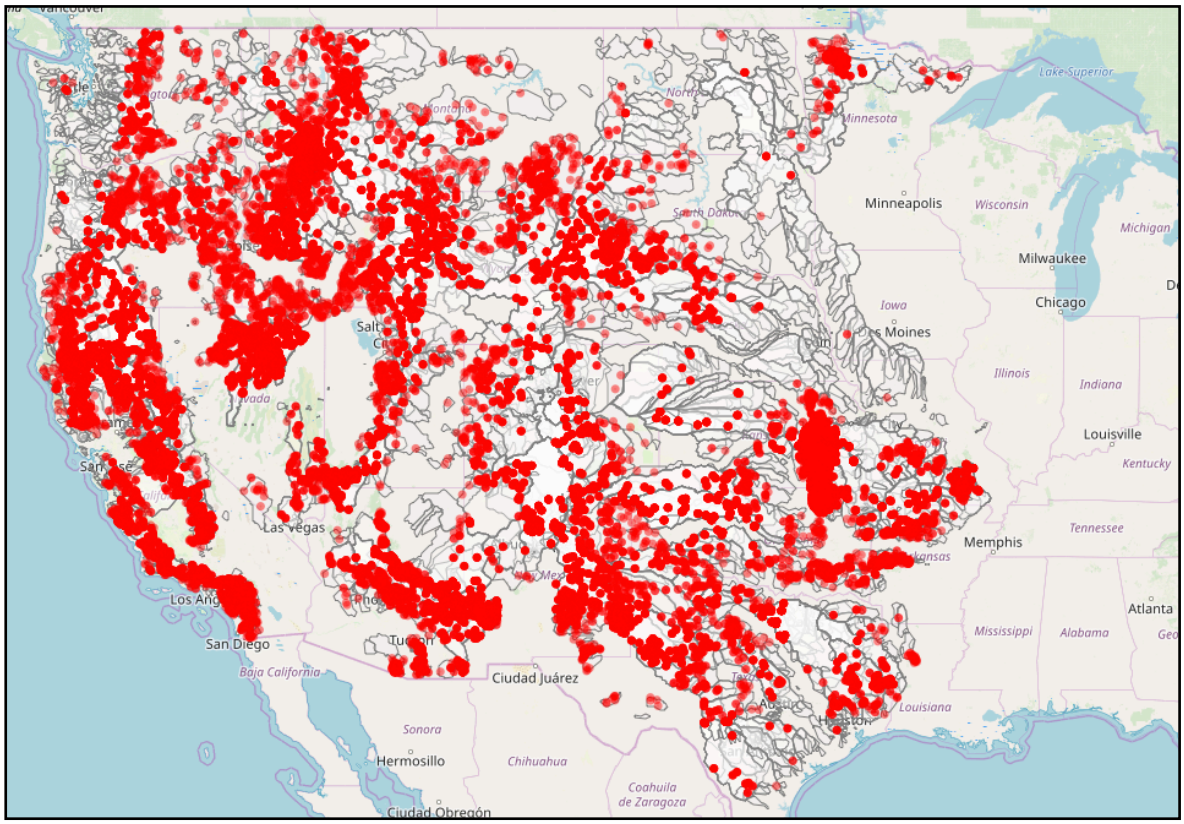

Figure 1. Western U.S. Study Domain: *All wildfire ignition points (recorded 1985-2016) are shown in red (Eidenshink et al., 2007). All GAGES-II basins are also displayed (Falcone, 2017). Note that some basins are nested.*

MTBS data were coupled with USGS GAGES-II basin information, and USGS National Water Information System (NWIS) stream gage data to support this regional analysis. Merging these datasets yielded a total of 255 wildfires across 187 gaged basins that have been observed for both streamflow and sediment, representing the wildfires and basins analyzed in the first section of this paper.

A single basin was isolated in order to evaluate and refine the methodology for quantifying post-fire sediment signals. This site was selected from the total 187 gaged basins based on several criteria that were established to identify a basin with the greatest likelihood of signal detection. These criteria include: minimal upstream regulation (e.g. dam density and storage) from GAGES-II, number of observed fires, size of observed fires as a percentage of basin size, and excluding non-snowmelt-dominated basins given

complexities associated with snowmelt timing and transport uncertainty. This selection process yielded the USGS Gage 08353000 for Rio Puerco near Bernardo, NM as the most suitable candidate. A plot of the study site is shown below in Figure 2. Located west of Albuquerque, NM, this location offers comparatively little infrastructure development, with a basin area of 15,724.93 km^2, 23 dams total (0.15 dams/km^2), and a dam storage density of 3.9 ML/km^2.

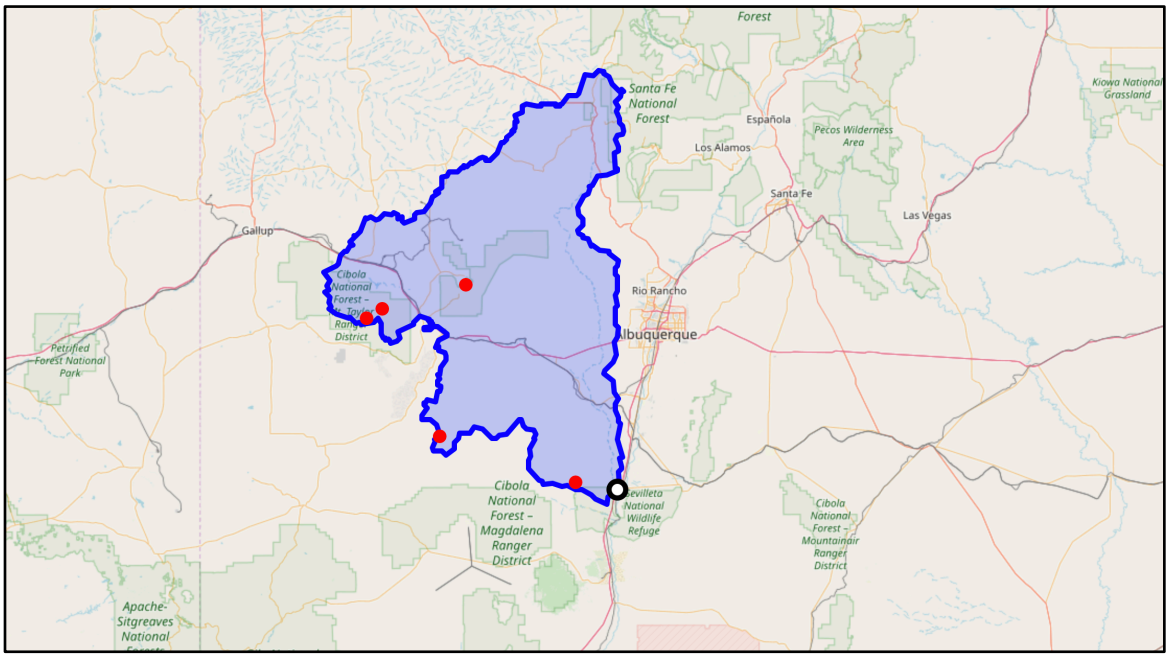

Figure 2. USGS Gage 08353000 (Rio Puerco near Bernardo, NM): *Basin extent is shown in blue. Fires observed for both sediment and streamflow are shown in red, and the gage location can be seen towards the south as a black and white circle.*

A total of 5 fires (2 prescribed burns and 3 wildfires) were observed within the drainage area during the period 1999-2014 when the gage was collecting both streamflow and sediment data. The largest fire, which occurred June 12th, 2004, consumed approximately 37.4 km^2 (0.23%) of the basin areal extent. The second and third largest fires occurred May 30th, 2008 and June 3rd, 1999, respectively, consuming 17.8 km^2 (0.11%) and 13.1 km^2 (0.08%) of the basin extent.

Streamflow and SSC data were available for the period between 1994 and 2016, with a brief period of streamflow only in 2015. A plot of observational data for the basin is shown below in Figure 3.

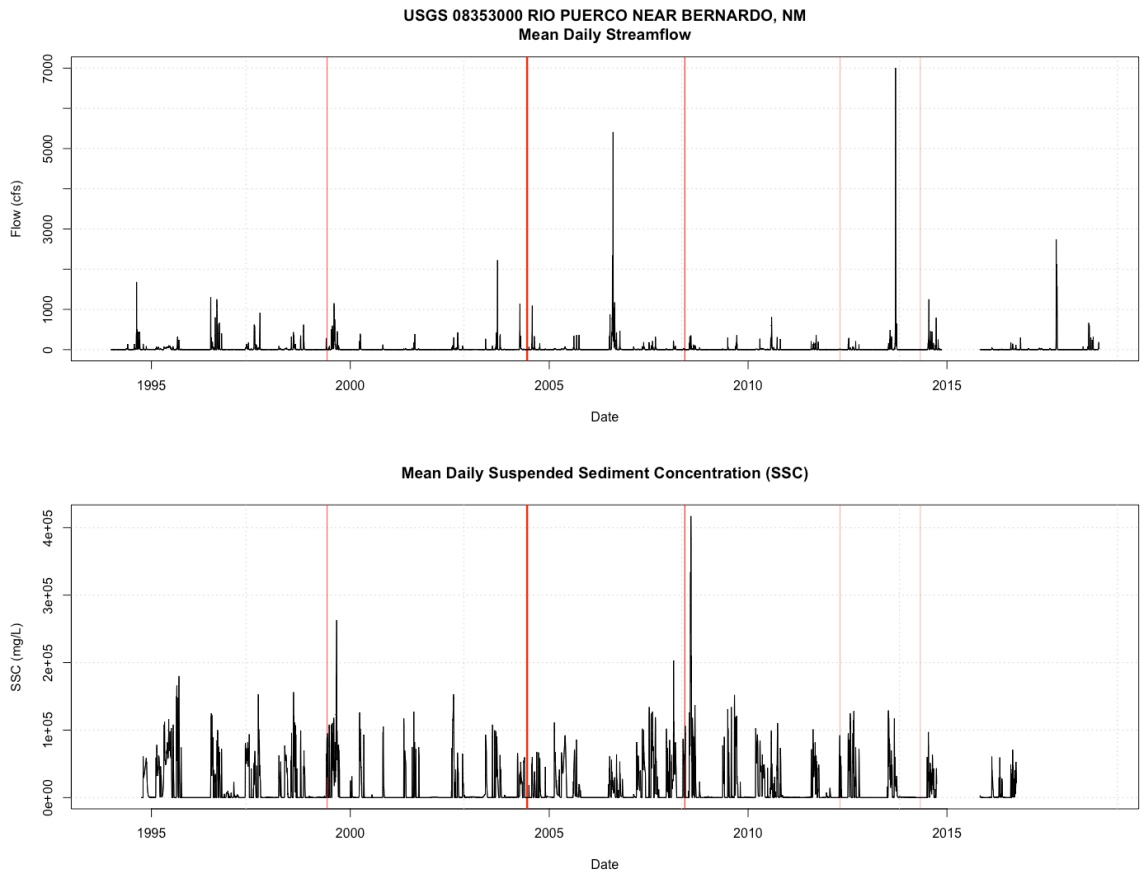

Figure 3. Mean daily streamflow (top) and mean daily SSC (bottom) data*. Vertical red bars denote wildfire ignition dates, with the thickness of the bars representing the relative size of the fires as a fraction of the total basin area.*

For the single site analysis, daily gridded 1-km precipitation data from Daymet (Thornton, et al., 2018) were utilized in addition to the gage data. These precipitation data were incorporated into the analysis in two ways: lumped over the basin areal extent to obtain a mean areal precipitation (MAP), and lumped individually over wildfire extents so as to only capture precipitation falling on fire-affected areas.

Methods

The Monovariate Rating Curve (MRC), also known as the sediment rating curve, is an empirical method for estimating sediment loading exclusively as a function of streamflow. The most common form is that of a power relationship:

$$SSL = aQ^b \tag{1}$$

where SSL is suspended sediment loading, Q is streamflow, a is a coefficient for the intercept, and b is an exponent for slope (Gray & Simoes, 2008). USGS daily streamflow

and sediment data were fitted to this model in order to create a summary relationship characterizing the expected sediment loading per unit streamflow for all 187 suitable basins with available data. This fitting process is demonstrated in Figure 4.

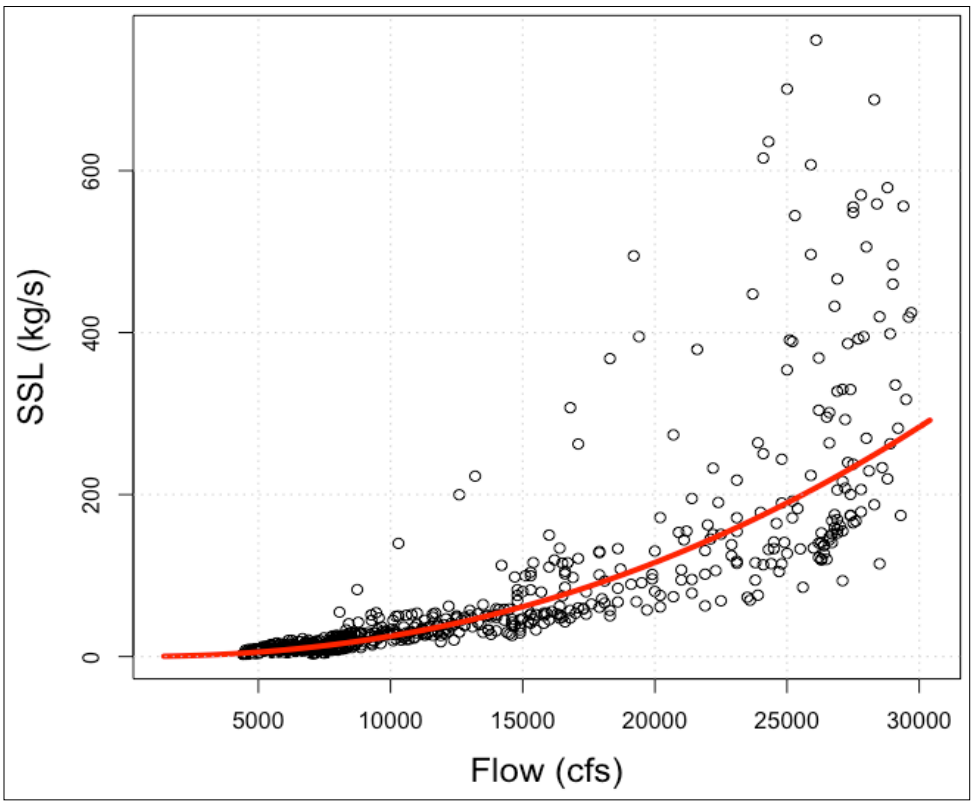

Figure 4. Sediment rating curve fitting: *An exponential relationship between SSL and Q is found and logged along with its correlation coefficient (R^2). The fitted coefficients are compiled along with GAGES-II basin properties for the wildfire analysis.*

Basin mean slope, relief ratio, drainage area, and total reservoir storage collected from the GAGES-II dataset were compiled along with fitted rating curve parameters to develop a profile for each basin, which were then used to select an appropriate study area for the single-site analysis.

A cascade of increasingly data-intensive techniques for detection of a post-wildfire signal was applied to the single site in New Mexico, with the intent of both *conclusively attributing*, and later *accurately predicting*, the presence and magnitude of a suspended sediment response at a basin outlet due to a wildfire event. The framework of this methodology is founded on two key motivations: the necessity for actionable post-fire sediment response information under conditions of data scarcity, and the need to identify influences on sediment response that may be generalized to the U.S. West region, such that inferences about post-fire sediment loading may be drawn for basins without an abundance of observational data. The most optimal technique would achieve an accurate prediction of sediment response magnitude due to a wildfire event using as little input data as possible.

The first method analyzes streamgage time-series data alone using a statistical technique called intervention analysis. Intervention analysis is commonly used to uncover the effects of an intervention, or an impactful event, on a time-series. Typically, an

AutoRegressive Integrated Moving Average (ARIMA) model (Box & Jenkins, 1976) is applied to pre-event time-series data and used to forecast theoretical post-event data. This essentially contrasts the actual post-event observations with the model scenario in which pre-event data are used to forecast post event response as if the event did not occur. An ARIMAX model is an extended version of ARIMA, and additionally includes one or more exogenous predictor variables. The equation for ARIMAX can be written as follows:

$$Y_t = C + v(B)X_t + N_t \tag{2}$$

where Y_t represents the dependent variable, X_t is the independent variable, C is the constant term, N_t is the stochastic disturbance (i.e. the 'noise'), B is the backshift operator, and $v(B)X_t$ is the transfer function that allows X to influence Y through a distributed lag (Peter & Silvia, 2012). The transfer function can then be described as:

$$v(B)X_t = (v_0 + v_1 B + v_2 B^2 + \cdots)X_t \tag{3}$$

This model was applied individually to each of the five wildfires at the study basin to train the model. The 'pre-fire' period used for training was defined as the start of the observational record up to the fire date of ignition. Determination of model parameters, including the lag order (number of lagged observations), degree of differencing (the number of times raw observations were differenced to remove nonstationarity), and the moving average order (the size of the moving average window), hereafter referred to as the variables (p, d, q), were made using the entirety of the observational record through step-wise Akaike Information Criterion (AIC) model ranking provided in the R function *auto.arima()* from the *forecast* package (Hyndman et al., 2019). A forecasted period of one year was selected to encapsulate a full post-fire season.

The second technique adds daily precipitation data from Daymet to create a basin mean areal precipitation as another predictor variable for the ARIMAX model. Several studies (Knapen, et al., 2007; Moody, et al., 2008; Momm, et al., 2018) identify precipitation intensity thresholds that must be overcome for the initiation of concentrated erosion and debris flows. Identifying this threshold may be particularly important for the prediction of suspended sediment following a fire, as a signal may not be readily detectable for storm events below these thresholds, whereas disproportionately high volumes of sediment may be transported during the first post-fire storm above the threshold. Initially, precipitation intensity was plotted against post-fire streamgage SSL to find evidence of this threshold by inspection. Then, precipitation data were used to filter out days during which no precipitation occurred (as it is assumed no overland flow was present to transport sediment into the channel), and subsequently added as a predictor variable for the ARIMAX model.

The third technique retains the spatial information of the precipitation data, rather than aggregating over the basin area. Fire extents from MTBS for the five events were compared against the gridded storm extents to find storms co-located with affected areas. A detectable signal may be more easily found and isolated when knowledge of whether a storm precipitated over a burned area is added. Thus, periods of time when no precipitation occurred over a wildfire-affected area were filtered out, and the remaining data were again modeled to detect pre- vs. post-fire differences in SSL.

Results

Regional Analysis

The results of fitting the MRC to observational data are summarized below. Figure 5 summarizes coefficient 'a' across the domain.

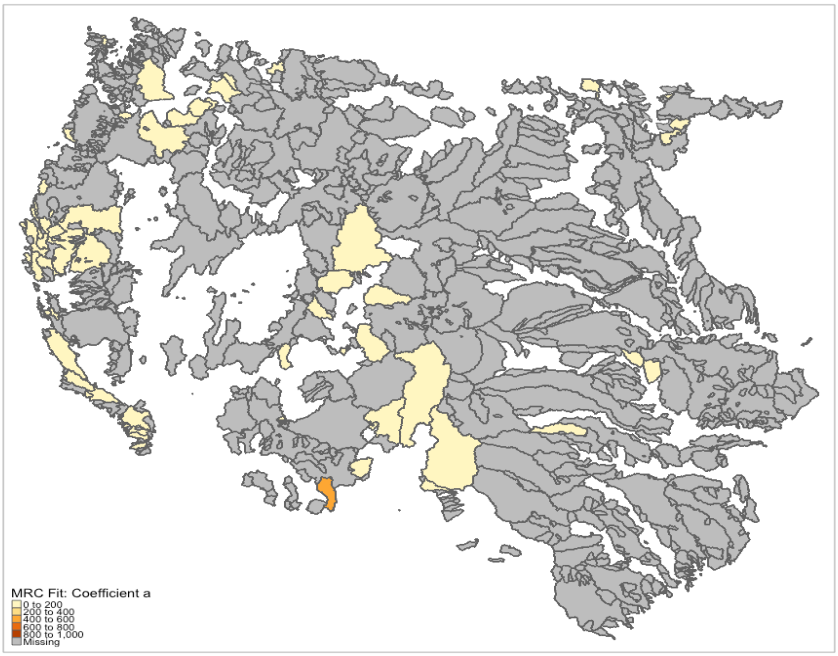

Figure 5. Spatial summary of coefficient 'a' from the MRC curve fitting process. *GAGES-II basins across the U.S. West are shown. Grayed-out basins are those with not enough available data.*

The spatial variation of exponent 'b' is shown below in Figure 6.

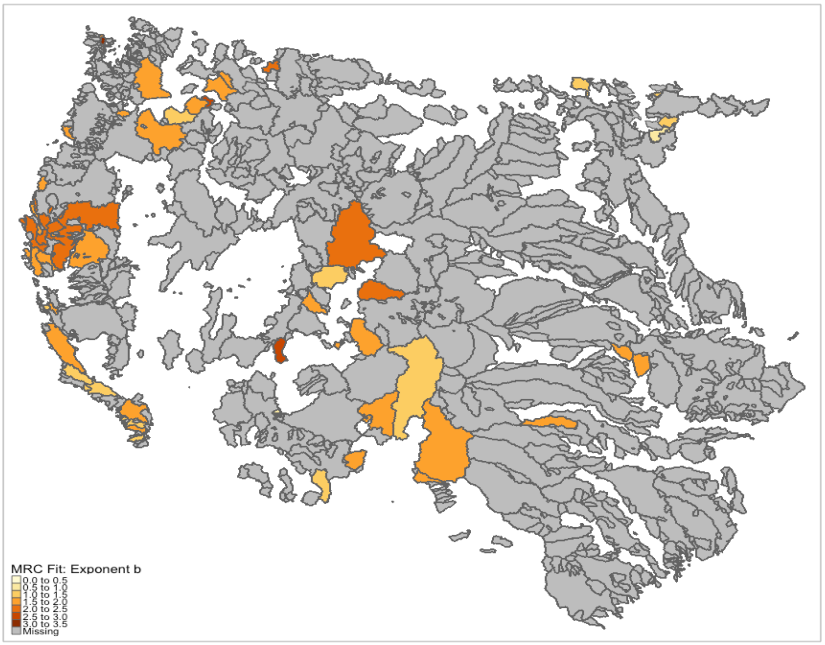

Figure 6. Spatial summary of exponent 'b' from the MRC curve fitting process. *GAGES-II basins across the U.S. West are shown. Grayed-out basins are those with not enough available data.*

Finally, the correlation coefficient, or R^2, of the fit between MRC-predicted and observed sediment is shown below in Figure 7.

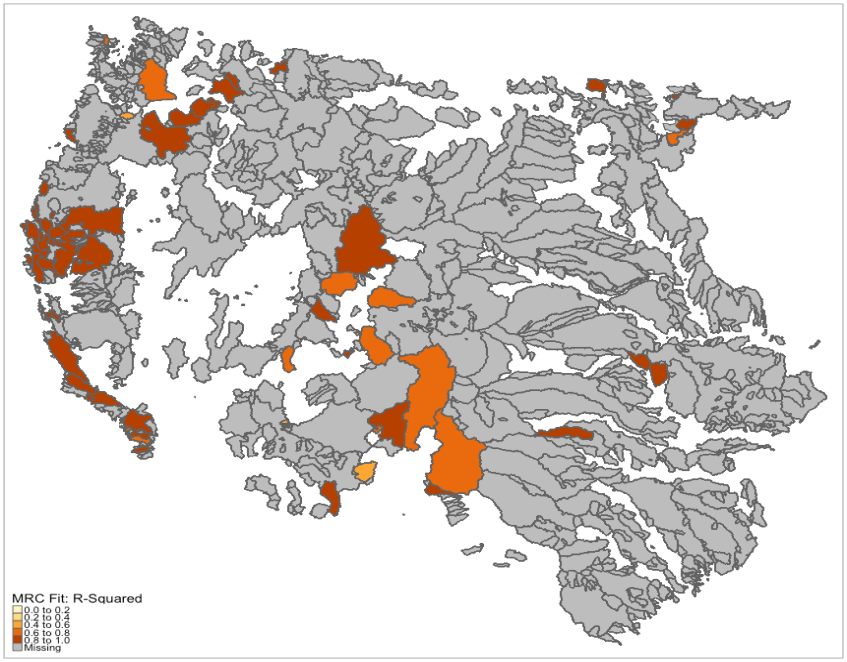

Figure 7. Spatial summary of exponent 'b' from the MRC curve fitting process. *GAGES-II basins across the U.S. West are shown. Grayed-out basins are those with not enough available data.*

The MRC fit was largely skilled across the domain for all 187 basins, with 140 basins showing an R-squared greater than 0.75. Coefficient 'a' remained relatively low

across all basins, likely indicative of the 'flashy' nature of streams located in the arid West. Results for exponent 'b' are arguably the most interesting; high relative variability in its magnitude points towards basin-level differences that may be affecting its value. However, comparing 'b' against several basin metrics such as relief, mean slope, basin size, and mean flow (not shown) did not reveal any strong explanatory skill.

Single site analysis

For the single site analysis at Rio Puerco near Bernardo, NM, flow was multiplied with SSC to obtain SSL, which represents the volume of sediment flowing through the channel. Before fitting to an ARIMA model, these time-series were first examined for the presence of long-term trends and seasonality. An augmented Dickey-Fuller (ADF) test was applied to test for stationarity. The null hypothesis of non-stationarity over the time period was rejected with $p < 0.01$, indicating the absence of any longer-term trends that would need to be included in the model. To identify seasonal cycles in the data, plots of the auto-correlation function (ACF) and partial auto-correlation function (PACF) for SSL observations at the gage were examined (Figure 8).

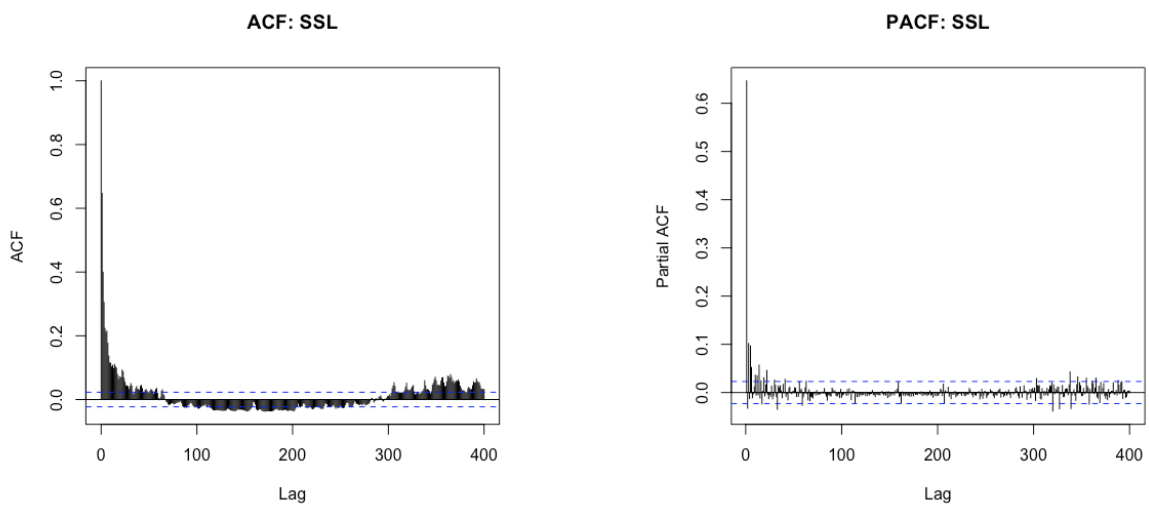

Figure 8. Autocorrelation function (left) and Partial autocorrelation function (right) for SSL. *The horizontal axis shows lag in days, and the vertical axis shows correlation.*

Significant auto-correlation exists for lags up to approximately one week, and, to a lesser extent, for a one-year lag, denoting the presence of an annual cycle for the time-series. A model optimization method using the R function 'auto.arima' was employed, which identifies a best model fit using the AIC method of ranking a model based on relative quality. Using the ARMIAX model with streamflow as an additional predictor, a non-seasonal AR order, degree of differencing, and MA order (p, d, q) = (2, 1, 2) was identified as the top performer through AIC best model selection, using the full record of observations.

For each wildfire, the model was fit to the pre-fire data and used to forecast the full year following the event. This was then compared against the true observed series for those 12 months, and the mean difference was taken to be the effect of the wildfire event. The results of this process are presented below in Figure 9.

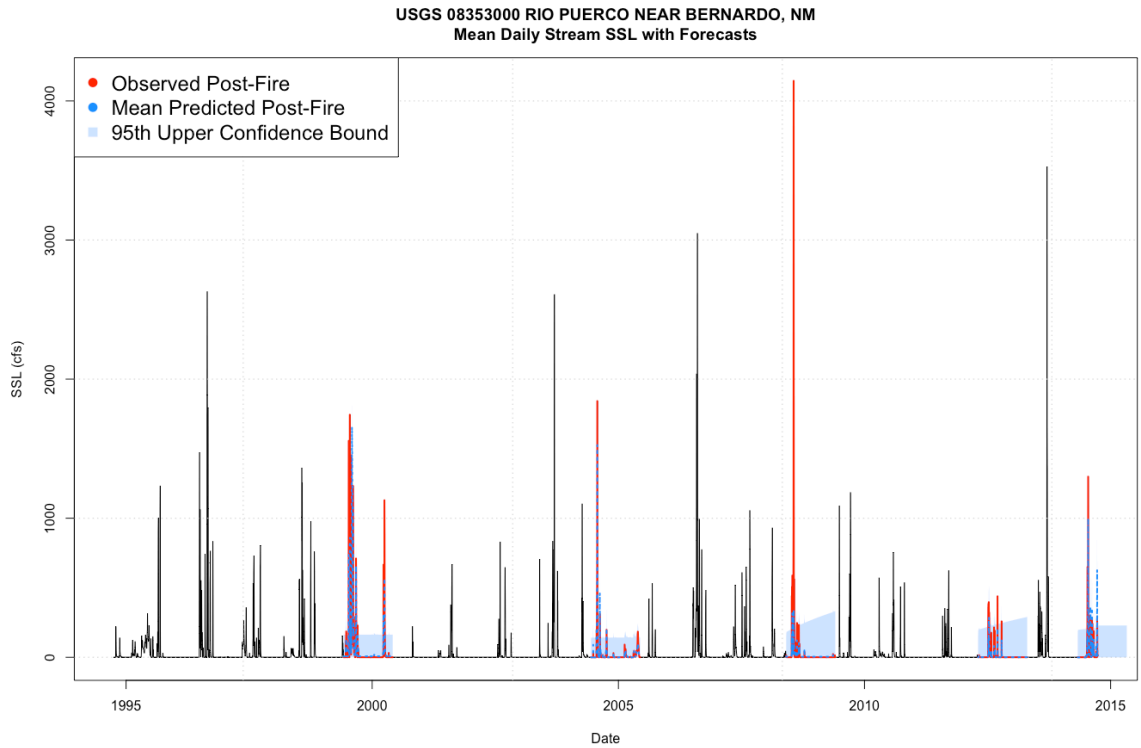

Figure 9. Model-predicted SSL versus observations following five observed wildfires at the study site near Bernardo, NM. *Pre-fire data used to inform the model is shown in black, the observed post-fire data is in red, model-predicted values are shown in blue, and the 95th percentile upper confidence bound is shown in light blue.*

Differences between post-fire observational and forecasted SSL during each post-fire year-long period are summarized below in Table 1.

Table 1. Summary of mean and maximum differences between forecast mean and observed SSL (in kg/s) during post-fire periods. *Ignition date and fire spatial extent are presented in the first column. Percent differences between forecasted and observed are also shown. An asterisk (*) denotes prescribed fires.*

Fire Event	Forecasted Mean SSL	Observed Mean SSL	Percent Difference	Forecasted Maximum SSL	Observed Maximum SSL	Percent Difference
1999-06-03 (13.15 km^2)	70.82	77.16	**8.22%**	1656.86	1744.32	**5.01%**
2004-06-12 (37.40 km^2)	20.02	20.63	**3.00%**	1525.73	1842.66	**17.20%**
2008-05-30* (17.83 km^2)	12.82	39.05	**67.17%**	340.74	4144.65	**91.78%**
2012-04-23 (6.4 km^2)	7.57	13.23	**42.78%**	288.75	439.03	**34.23%**
2014-05-02* (5.77 km^2)	49.07	56.83	**13.65%**	997.22	1299.03	**23.23%**

Next, the additional incorporation of precipitation data was tested to first determine if a specific post-fire erosion threshold could be found from the data, then added as a predictor to the ARIMAX model. First, a cross-correlation was applied between streamflow and precipitation, shown in Figure 10.

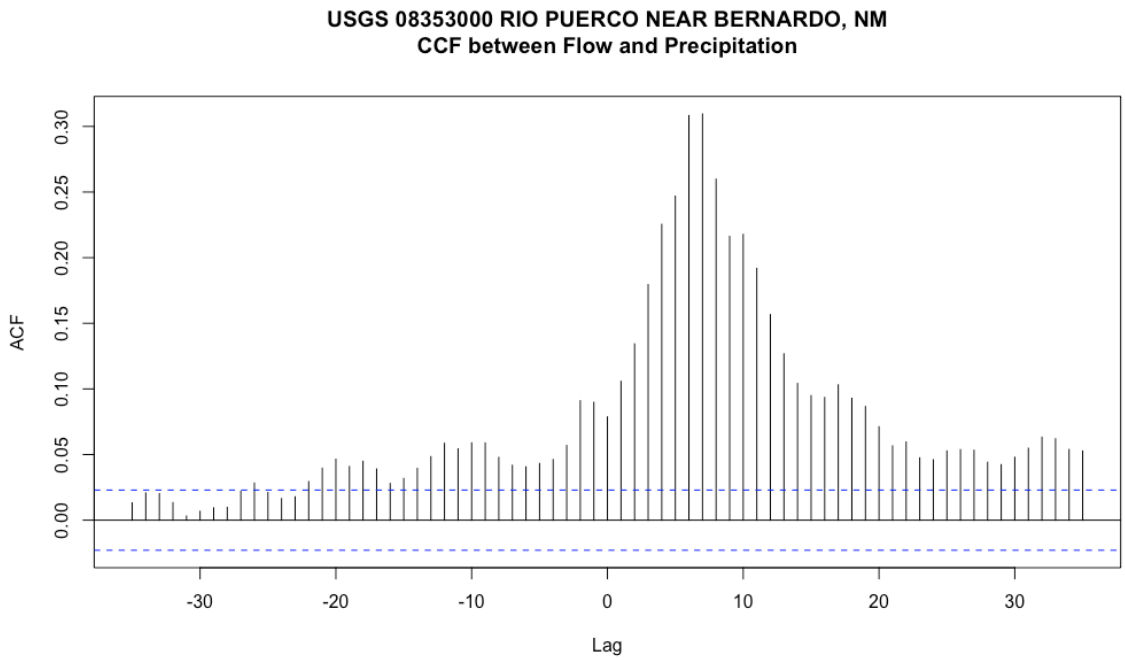

Figure 10. Cross-correlation between streamflow and precipitation. *The horizontal axis shows the lag in days between the two series of streamflow and precipitation. The vertical axis shows correlation.*

Prior literature, such as Valois et al. (2017), have taken the time of maximum correlation to be representative of the time of concentration for the watershed. The magnitude of the maximum correlation can also be taken as an indicator for the strength of the relationship between streamflow and precipitation. This basin shows a maximum lag time of 7 days, and a maximum correlation of 0.31, indicating a relatively slow concentration time and somewhat weak relationship between streamflow and precipitation. These initial findings point to the possibility of a predominantly groundwater discharge-fed watershed and/or the presence of other attenuating sub-basin processes that may store precipitation for a period of time before reaching the basin outlet.

Precipitation was fed into the ARIMAX model alongside streamflow as an exogeneous variable and used to forecast over the same post-fire periods. Adding precipitation as an additional parameter did not yield any significantly different forecast predictions, reflecting the weakness of basin-averaged precipitation as a predictor for SSL at the basin outlet. Among all fires, the largest difference between post-fire predicted mean SSL from the model with and without precipitation added was 0.71 kg/s. The largest difference in maximum SSL was 6.52 kg/s.

Finally, only precipitation that fell over a fire-affected area were analyzed. For each fire event, a unique time series of precipitation was used that represented precipitation falling within the extent of the fire perimeter provided by MTBS data. In order to determine if a sediment signal at the basin outlet could be attributed to sediment delivered from a burned area, the top 10 largest instantaneous SSL magnitudes were examined for

each post-fire period. Cumulative precipitation that had fallen within the prior week (based on the estimated 7-day time of concentration for this basin) were plotted against the largest SSL magnitudes during the post-fire seasons (Figure 11).

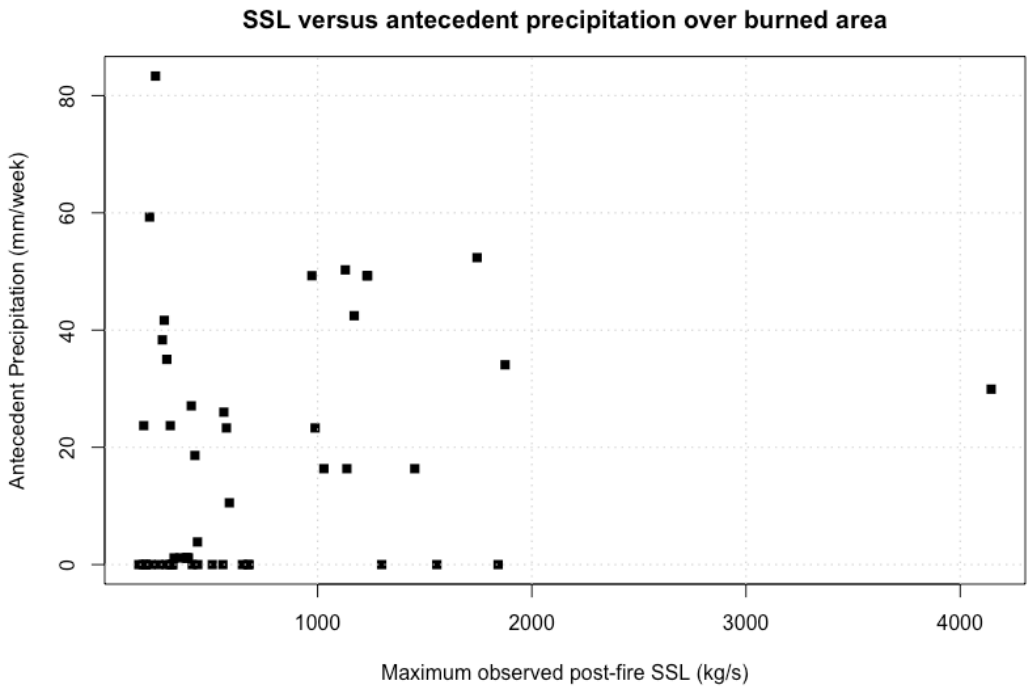

Figure 11. Cumulative precipitation over burned areas from the week preceding maximum observed SSL responses during post-fire periods. *For each wildfire event, the top 10 post-fire SSL magnitudes were identified. For the week prior to these observations, precipitation over the burned area were summed. These SSL magnitudes and accumulated precipitation are shown.*

Of the 50 maximum instantaneous sediment loadings (10 for each of 5 observed fires in the basin), 20 showed no prior precipitation over the burned area, indicating that at least 40% of these large sediment signals could not be attributed to sediment originating from burned areas.

Replacing precipitation over the entire basin with precipitation over burned areas alone again yielded few differences from the original model. Among all fires, the largest difference between post-fire predicted mean SSL from the model with and without burned area precipitation added was 1.28 kg/s. The largest difference in maximum SSL was 21.07 kg/s.

Preliminary Conclusions and Future Work

In this paper, we sought to characterize streamflow and sediment relationships through commonly used rating curve parameters at a diverse set of gaged locations across the western United States. We applied a statistical model to pre-fire streamgage data and forecasted the post-fire season, comparing differences in suspended sediment loading (SSL) magnitudes between the forecast and observations, and later adding data from

Daymet (basin-averaged, then gridded) and MTBS to improve post-fire sediment signal strength.

The regional analysis revealed trends in the rating curve exponent ‘b’ that may be worthwhile in future work to investigate further in order to identify correlations with additional basin characteristics not analyzed here. Future work will explore other predictive variables, such as land cover, geology, and climate, and their covariance with the value of ‘b’.

For the single-site analysis, the gage-only method showed post-fire sediment signal for several of the fires, based on the difference between the observed and forecasted time series. The presence of these differences are encouraging, and reveal the potential for establishing an estimate of post-fire sediment response based on gage data alone. However, data limitations would make this method difficult, as most gages do not provide consistent sediment measurements. Including precipitation did not significantly affect the model; however, examining the link between cross-correlation in streamflow and precipitation versus sediment response may be worthwhile to investigate, as it could be posited that a shorter time of concentration, paired with a high correlation between precipitation and streamflow, may be indicative of a well-connected basin capable of delivering sediment with relative efficiency. Underpinning this hypothesis is the notion that a well-connected basin with little attenuation of streamflow from storm to outlet may also offer fewer obstacles for sediment as well. In these cases, strong post-fire SSL magnitudes may be more common.

Future work will focus on the development and application of a more sophisticated sediment routing model, which can explicitly take into account sediment traps and other sub-basin processes that may help or hinder the journey of a sediment particle from a burned area to the outlet.

References

Benavides-Solorio, J., MacDonald, L.H., 2001. Post-fire runoff and erosion from simulated rainfall on small plots, Colorado Front Range. Hydrol. Process. 15, 2931–2952. https://doi.org/10.1002/hyp.383

Blake, W.H., Droppo, I.G., Humphreys, G.S., Doerr, S.H., Shakesby, R.A., Wallbrink, P.J., 2007. Structural characteristics and behaviour of fire-modified soil aggregates. Journal of Geophysical Research 112, F02020.

Blake, W.H., Wallbrink, P.J., Droppo, I.G., 2009. Sediment aggregation and water quality in wildfire-affected river basins. Mar. Freshwater Res. 60, 653–659. https://doi.org/10.1071/MF08068

Box, G. E. P and Jenkins, G.M., (1976). "Time series analysis: Forecasting and control," Holden-Day, San Francisco.

Brunsden, D., Thornes, J.B., 1979. Landscape sensitivity and change. Transactions of the Institute of Geographers, New Series 4, 463 – 484.

Cerdá, A., Doerr, S.H., 2005. Influence of vegetation recovery on soil hydrology and erodibility following fire: an 11-year investigation. International Journal of Wildland Fire 14, 423. https://doi.org/10.1071/WF05044

Emmerich, W.E., Cox, J.R., 1994. Changes in Surface Runoff and Sediment Production after Repeated Rangeland Burns. Soil Science Society of America Journal 58, 199–203. https://doi.org/10.2136/sssaj1994.03615995005800010029x

Falcone, J.A., 2017, U.S. Geological Survey GAGES-II time series data from consistent sources of land use, water use, agriculture, timber activities, dam removals, and other historical anthropogenic influences: U.S. Geological Survey data release, https://doi.org/10.5066/F7HQ3XS4.

Ferguson, H.F., Hamel, J.V., 1981. Valley Stress Relief In Flat-lying Sedimentary Rocks. Presented at the ISRM International Symposium, International Society for Rock Mechanics and Rock Engineering.

Fernández, C., Vega, J.A., Jiménez, E., Fonturbel, T., 2011. Effectiveness of three post-fire treatments at reducing soil erosion in Galicia (NW Spain). Int. J. Wildland Fire 20, 104–114. https://doi.org/10.1071/WF09010

Fryirs, K., 2013. (Dis)Connectivity in catchment sediment cascades: a fresh look at the sediment delivery problem. Earth Surface Processes and Landforms 38, 30–46. https://doi.org/10.1002/esp.3242

Fryirs, K., Brierley, G.J., 2001. Variability in sediment delivery and storage along river courses in Bega catchment, NSW, Australia: implications for geomorphic river recovery. Geomorphology 38, 237–265. https://doi.org/10.1016/S0169-555X(00)00093-3

Gray JR, Simões FJM (2008) Estimating sediment discharge. In: Marcelo G (ed) Sedimentation engineering—processes, measurements, modeling, and practice. American Society of Civil Engineers Manual 110, Appendix D, pp. 1065–1086. http://water.usgs.gov/ osw/techniques/Gray_Simoes.pdf

Hyndman R, Athanasopoulos G, Bergmeir C, Caceres G, Chhay L, O'Hara-Wild M, Petropoulos F, Razbash S, Wang E, Yasmeen F (2019). *forecast: Forecasting functions for time series and linear models*. R package version 8.5, http://pkg.robjhyndman.com/forecast.

Johansen, M.P., Hakonson, T.E., Breshears, D.D., 2001. Post-fire runoff and erosion from rainfall simulation: contrasting forests with shrublands and grasslands. Hydrol. Process. 15, 2953–2965. https://doi.org/10.1002/hyp.384

Jones, K.W., Cannon, J.B., Saavedra, F.A., Kampf, S.K., Addington, R.N., Cheng, A.S., MacDonald, L.H., Wilson, C., Wolk, B., 2017. Return on investment from fuel treatments to reduce severe wildfire and erosion in a watershed investment program in Colorado. Journal of Environmental Management 198, 66–77. https://doi.org/10.1016/j.jenvman.2017.05.023

Knapen, A., Poesen, J., Govers, G., Gyssels, G., Nachtergaele, J., 2007. Resistance of soils to concentrated flow erosion: A review. Earth-Science Reviews 80, 75–109. https://doi.org/10.1016/j.earscirev.2006.08.001

Luis, M.D., González-Hidalgo, J.C., Raventós, J., 2003. Effects of fire and torrential rainfall on erosion in a Mediterranean gorse community. Land Degradation & Development 14, 203–213. https://doi.org/10.1002/ldr.547

Meyer, G.A., Wells, S.G., 1997. Fire-related sedimentation events on alluvial fans, Yellowstone National Park, U.S.A. Journal of Sedimentary Research 67, 776–791. https://doi.org/10.1306/D426863A-2B26-11D7-8648000102C1865D

Momm, H.G., Wells, R.R., Bennett, S.J., 2018. Disaggregating soil erosion processes within an evolving experimental landscape. Earth Surface Processes and Landforms 43, 543–552. https://doi.org/10.1002/esp.4268

Moody, J.A., Martin, D.A., Cannon, S.H., 2008. Post-wildfire erosion response in two geologic terrains in the western USA. Geomorphology 95, 103–118. https://doi.org/10.1016/j.geomorph.2007.05.011

Moody, J.A., Martin, D.A., 2001. Initial hydrologic and geomorphic response following a wildfire in the Colorado Front Range. Earth Surf. Process. Landf. 26, 1049–1070. https://doi.org/10.1002/esp.253

Neary, D.G., Koestner, K.A., Youberg, A., 2011. Hydrologic Impacts of High Severity Wilidfire: Learning from the Past and Preparing for the Future. 24th Annual Symposium of the Arizona Hydrological Society; Watersheds near and far: Response to changes in climate and landscape; September 18-20, 2010; Flagstaff, AZ. 8 p.

Pelletier, J.D., Orem, C.A., 2014. How do sediment yields from post-wildfire debris-laden flows depend on terrain slope, soil burn severity class, and drainage basin area? Insights from airborne-LiDAR change detection. Earth Surface Processes and Landforms 39, 1822–1832. https://doi.org/10.1002/esp.3570

Reneau, S.L., Katzman, D., Kuyumjian, G.A., Lavine, A., Malmon, D.V., 2007. Sediment delivery after a wildfire. Geology 35, 151–154. https://doi.org/10.1130/G23288A.1

Rowe, P. B., Influence of Woodland Chaparral on Water and Soil in Central California, California Department of Natural Resources, Division of Forestry, 70 pp., 1948.

Sankey, J.B., Kreitler, J., Hawbaker, T.J., McVay, J.L., Miller, M.E., Mueller, E.R., Vaillant, N.M., Lowe, S.E., Sankey, T.T., 2017. Climate, wildfire, and erosion ensemble foretells more sediment in western USA watersheds. Geophysical Research Letters 44, 8884–8892. https://doi.org/10.1002/2017GL073979

Shakesby, R.A., Doerr, S.H., 2006. Wildfire as a hydrological and geomorphological agent. Earth-Science Reviews 74, 269–307. https://doi.org/10.1016/j.earscirev.2005.10.006

Smith, H.G., Sheridan, G.J., Lane, P.N.J., Nyman, P., Haydon, S., 2011. Wildfire effects on water quality in forest catchments: A review with implications for water supply. Journal of Hydrology 396, 170–192. https://doi.org/10.1016/j.jhydrol.2010.10.043

Swanson, F J. 1981. Fire and geomorphic processes. Pages 401-420 in Proceedings of the Conference on Fire Regimes and Ecosys- tem Properties. USDA Forest Service Gener- al Technical Report WO-26, Washington, DC.

Thornton, P.E., M.M. Thornton, B.W. Mayer, Y. Wei, R. Devarakonda, R.S. Vose, and R.B. Cook., 2018. Daymet: Daily Surface Weather Data on a 1-km Grid for North America, Version 3. ORNL DAAC, Oak Ridge, Tennessee, USA. https://doi.org/10.3334/ORNLDAAC/1328

Valois, R., Vouillamoz, J.-M., Lun, S., Arnout, L., 2017. Assessment of water resources to support the development of irrigation in northwest Cambodia: a water budget approach. Hydrological Sciences Journal 62, 1840–1855. https://doi.org/10.1080/02626667.2017.1351030

Vieira, D.C.S., Fernández, C., Vega, J.A., Keizer, J.J., 2015. Does soil burn severity affect the post-fire runoff and interrill erosion response? A review based on meta-analysis of field rainfall simulation data. Journal of Hydrology 523, 452–464. https://doi.org/10.1016/j.jhydrol.2015.01.071

Wondzell, S.M., King, J.G., 2003. Postfire erosional processes in the Pacific Northwest and Rocky Mountain regions. Forest Ecology and Management, The Effect of Wildland Fire on Aquatic Ecosystems in the Western USA. 178, 75–87. https://doi.org/10.1016/S0378-1127(03)00054-9